340
4/30/81

T.S.

②

Dr. 2598

COO-3001-4

DEVELOPMENT OF HIGH EFFICIENCY, LOW COST $ZnSiAs_2$ SOLAR CELLS

RTI Project 41U-1803

Quarterly Technical Progress Report No. 4 for January 1—March 31, 1980

By
J. E. Andrews

MASTER

Dist-252
NTIS-22

Work Performed Under Contract No. AC04-79ET23001

Research Triangle Institute
Research Triangle Park, North Carolina

U.S. Department of Energy

Solar Energy

DISCLAIMER

COO-3001-4
Distribution Category UC-63e

DEVELOPMENT OF HIGH EFFICIENCY, LOW COST $ZnSiAs_2$ SOLAR CELLS

RTI Project 41U-1803

Quarterly Technical Progress Report No. 4

for

U. S. Department of Energy

Contract No. DE-AC04-79ET23001

January 1, 1980 to March 31, 1980

J. E. Andrews, Principal Investigator
Research Triangle Institute
P. O. Box 12194
Research Triangle Park, N. C. 27709

ABSTRACT

The p-$ZnSiAs_2$/n-GaAs structures fabricated earlier were analyzed using the Electron Beam Induced Current technique and were found to have a diffused p-n junction in the GaAs. The short circuit current density associated with this structure was found to be a factor of 2 to 3 lower than predicted when analyzed as a $ZnSiAs_2$/GaAs heteroface structure (the $ZnSiAs_2$ was assumed to behave as a window layer).

Epitaxial growth has now been demonstrated for two additional substrates, Si and α-Al_2O_3. In the case of Si, it was necessary to first grow a Si epi-layer followed by $ZnSiAs_2$ growth. Heretofore, epitaxial growth of $ZnSiAs_2$ has only been reported on Ge and GaAs substrates.

n-$ZnSiAs_2$/p-Si structures have been fabricated which exhibit photovoltaic behavior. It is not clear yet whether the photovoltaic behavior is due to a diffused junction in the Si or is indicative of a true heterostructure behavior.

$ZnSiAs_2$ p-n junction formation continues to be investigated but as yet has not resulted in junction behavior.

1.0 INTRODUCTION

The effort during the past quarter was directed in part toward an analysis of the previously described p-$ZnSiAs_2$/n-GaAs structures using the Electron Beam Induced Current (EBIC) measurement technique and in part toward continuing the growth of $ZnSiAs_2$ on Si substrates under the conditions that led to the identification of the low carrier concentration n-$ZnSiAs_2$ deposits.

Earlier Hall Effect measurements that led to the identification of n-$ZnSiAs_2$ grown on n-Si substrates (100-400Ω-cm) were repeated growth on p-Si and α-Al_2O_3 substrates in order to simplify the interpretation of those measurements. The results again indicate that n-type layers were deposited plus the n-$ZnSiAs_2$/p-Si structure exhibited some photovoltaic behavior.

Several attempts were made at fabricating a p-n $ZnSiAs_2$ junction but as yet have not resulted in junction behavior. It appears that part of the problem may be due in part to the quality of the $ZnSiAs_2$ growth on the Si substrates.

The most significant development in the growth of $ZnSiAs_2$ is that there are two additional substrates, (111) Si and (0001) α-Al_2O_3, on which $ZnSiAs_2$ has now been grown epitaxially. Heretofore, $ZnSiAs_2$ layers grown on Si substrates were typically polycrystalline. More recently, by first growing a Si epitaxial layer, epitaxial $ZnSiAs_2$ was achieved on Si substrates.

2.0 TECHNICAL DISCUSSION

2.1 Evaluation of p-$ZnSiAs_2$/n-GaAs Structures Using EBIC

An electron beam induced current (EBIC) measurement capability has now been established using a Model 9DM Specimen Current Amplifier (SCA)* in conjunction with an ETEC Autoscan Scanning Electron Microscope (SEM). The current induced by the primary electron beam was brought out from the device terminals to the SCA. The SCA output was monitored and also fed into a manual video amplifier so that either intensity modulated, or y-modulated EBIC images could be produced. Also, EBIC line scans through selected portions of the sample can be obtained and superimposed on the secondary electron (SE) image.

Figure 1 shows a secondary electron image of the cross-section of a cleaved p-$ZnSiAs_2$/n-GaAs device (Sample No. 137C-6) with an EBIC line scan superimposed on the secondary image. As can be seen from the figure, the EBIC peak was 1.5 μm below the $ZnSiAs_2$/GaAs interface. The thickness of the $ZnSiAs_2$ is 2.0 μm for this sample. This leads to a Zn diffusion coefficient of 49.7 $\mu m^2/hr$ (1.38×10^{-10} cm^2/sec) in GaAs (background doping level of $8 \times 10^{16}/cm^3$) with $ZnSiAs_2$ as the Zn source at 650°C for 1 hour.

The sample shown here, discussed in the previous quarterly, gave an AMO short circuit current density of 6.5 ma/cm^2 and a conversion efficiency of 2.5% which is to be compared with a calculated short circuit density of 16 ma/cm^2.** The fill factor and open circuit voltage (.658 and .79 v) are somewhat lower than expected for a good GaAs junction and may be attributable in part to contact related problems.

---

*On loan from G&W Electronics, Atlanta, Ga.

**Calculations provided by North Carolina State University.

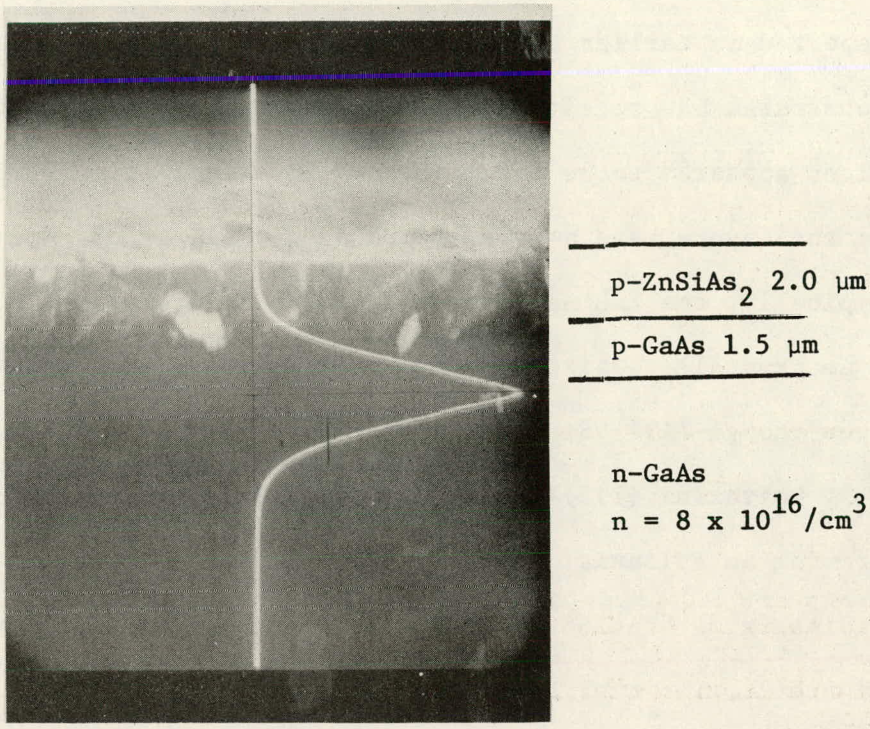

Figure 1. Secondary electron image of cross-sectional view of cleaved (along 110) p-ZnSiAs$_2$/n-GaAs structure. An EBIC linescan is shown superimposed on the image. The baseline was adjusted to correspond to the actual electron beam trace across the specimen. The p-GaAs region shown in the figure is due to the in-diffusion of Zn from the ZnSiAs$_2$ layer.

The calculated short circuit current density of 16 ma/cm^2 assumed a 10 μm electron diffusion length for the GaAs which, according to the EBIC data, is on the order of 1 μm. This would give a predicted short circuit current density more in line with the measured value.

2.2 Epitaxial Growth of $ZnSiAs_2$ on Si and α-Al_2O_3 Substrates

Epitaxial growth of $ZnSiAs_2$ on GaAs and Ge substrates has been reported in earlier reports. More recently, the growth of $ZnSiAs_2$ on Si substrates has received increased attention since the carrier concentrations appeared to be significantly lower and more importantly, a number of the layers were n-type according to Hall Effect and C-V measurements. Typically, the $ZnSiAs_2$ layers grown on Si are polycrystalline with 1 to 5 μm crystallite size and relatively strong (220) and (024) orientations even though (111) Si substrates were used.

Epitaxial (112) $ZnSiAs_2$ on (111) Si has now been deposited by first growing an epitaxial layer of (111) Si at 900°C followed immediately by $ZnSiAs_2$ growth at 655°C. The resulting diffraction pattern is shown in Figure 2. The quality of the epitaxial growth (structurally and morphologically speaking) does not yet appear to be quite as good as that obtained on 100 Ge substrates.

α-Al_2O_3 substrates* are currently being used in order to facilitate Hall Effect measurements. Epitaxial growth of (112) $ZnSiAs_2$ on (0001) α-Al_2O_3 has now been demonstrated as is evidenced by the x-ray diffraction pattern shown in Figure 3. The surfaces of these layers are very similar to those grown on Si substrates which are typically non-specular. Thus

---

*Epi-finished (0001) α-Al_2O_3 substrates purchased from Imasco, Inc., Quakertown, Pa.

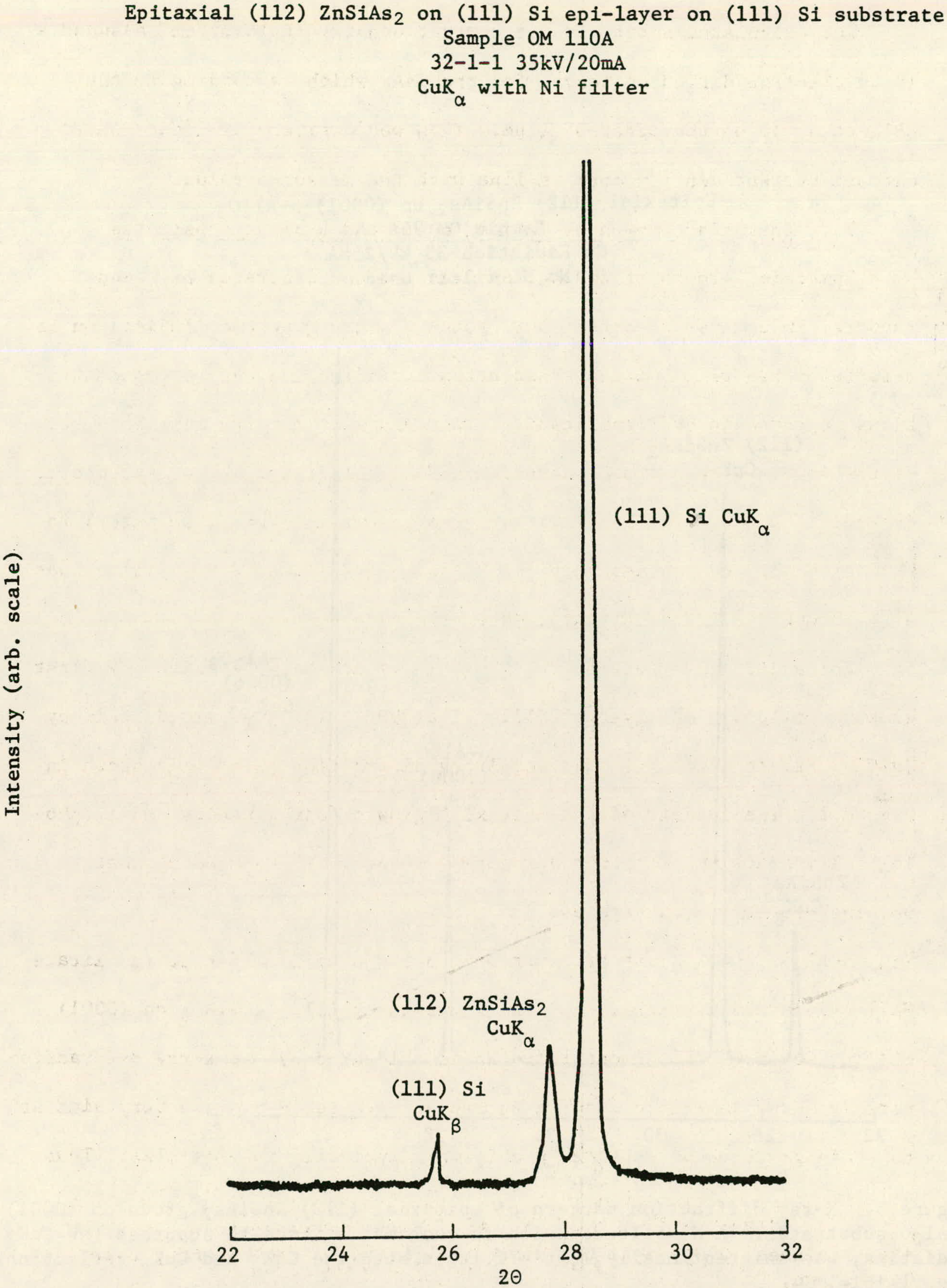

Figure 2. X-ray diffraction pattern epitaxial (112) ZnSiAs$_2$ grown on (111) Si substrates. This layer was grown by first growing an epitaxial layer of Si followed then by ZnSiAs$_2$. No other ZnSiAs$_2$ reflections were seen when scanned from 2Θ = 90° to 20°. CuK$_\alpha$ radiation was used for the analysis.

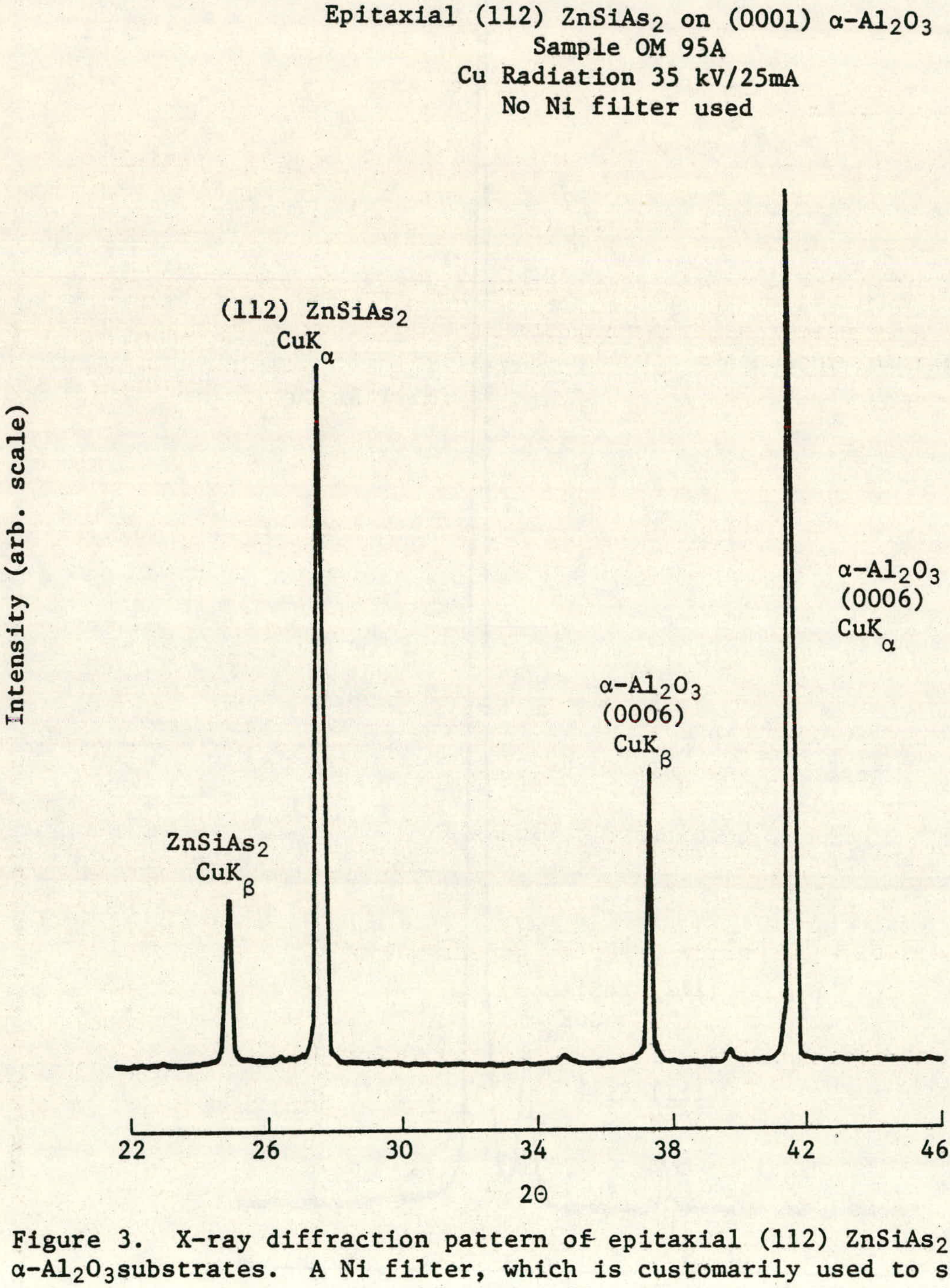

Figure 3. X-ray diffraction pattern of epitaxial (112) $ZnSiAs_2$ grown on (0001) α-Al_2O_3substrates. A Ni filter, which is customarily used to suppress the CuK_β radiation, was unintentionally left off, thus both the CuK_α and CuK_β reflections are visible.

far, mirror-like chalcopyrite layers have been obtained only on Ge and GaAs substrates.

Substrate preparation includes degreasing and an HF dip prior to insertion into the reactor for the Si substrates and degreasing only for the α-Al_2O_3 substrates.

2.3 Ohmic Contacts

A continuing problem is the fabrication of ohmic contacts, especially to the newer more lightly doped $ZnSiAs_2$ (grown on Si substrates). Typically, the contact structures used during the initial phase of the contact investigation are arrays of 15 mil dia. circular contacts spaced on 20 mil centers. This gives an active area of 44.2% of the total device area and permits examination of the uniformity of the characteristics across the sample.

V-I curves are typically obtained between pairs of the 15 mil dia. contacts (2.74×10^{-5} cm^2 per contact). The non-ohmic characteristics have typically fallen into two distinct classes. The first exhibits a high resistance at the origin and much lower resistance away from the origin. However, the second and most recent class exhibits just the opposite behavior, with the lower resistance portion of the curve at the origin (or 8 to 13KΩ) with much higher resistances (42 to 260KΩ) observed further away from the origin as is shown in Figure 4. The sample OM82A exhibited this behavior between two Ag/Sn contacts applied to an as-grown portion of the sample. In an effort to produce ohmic behavior, this contact structure was applied to a new portion of OM82A ($ZnSiAs_2$ on Si substrate) in which the surface had been etched in a buffered HF

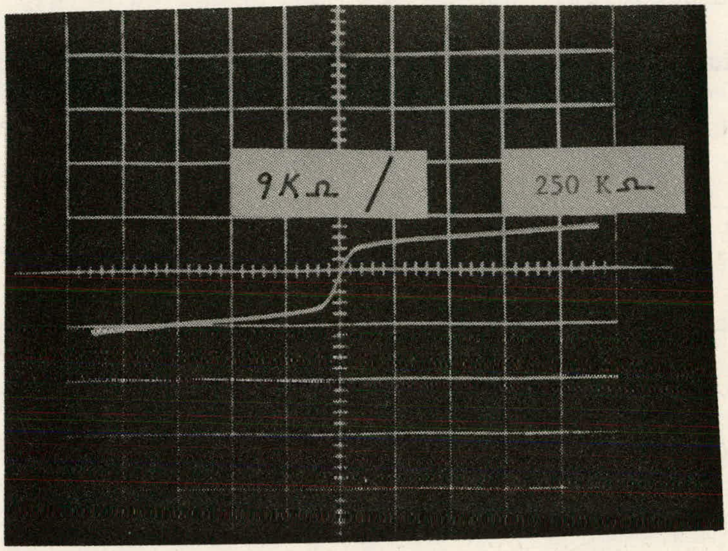

OM82A
without etching

V_F = 1 V/div

V_R = 1 V/div

I = 50 μa/div

Figure 4. Dark I-V curves for pair of 15 mil dia. Ag/Sn contacts vacuum evaporated onto as-grown $ZnSiAs_2$ surface. Surface preparation involved degreasing only.

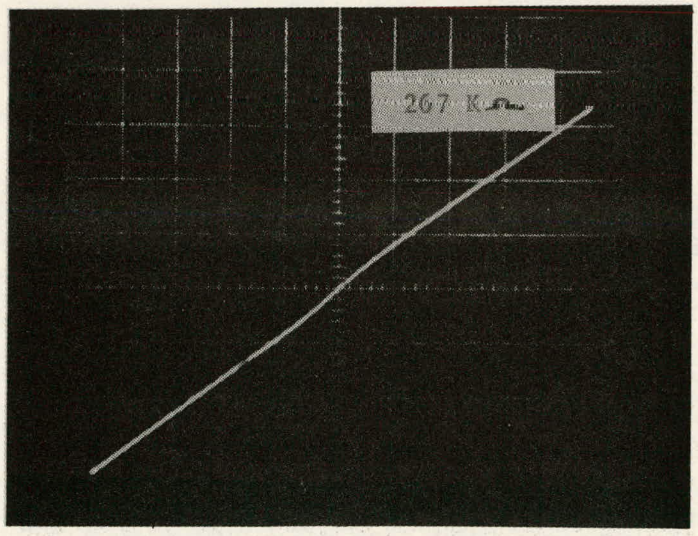

OM82A
with buffered HF
etching

V_F = 2 V/div

V_R = 2 V/div

I = 10 μa/div

Figure 5. Dark I-V curves for pair of 15 mil dia Ag/Sn contacts vacuum evaporated onto as-grown $ZnSiAs_2$ surface. Surface preparation included degreasing plus buffered HF etch immediately preceding contact evaporation.

solution. This did result in ohmic behavior but suprisingly with the higher of the two resistance regions observed in Figure 4 dominating the final resistance as is shown in Figure 5.

This non-ohmic behavior was thought to be related to the presence of an oxide layer, however, the V-I characteristics do not exhibit the high resistance region at the origin that is typical of the oxide problem.

Depth profiles have subsequently been obtained for epitaxial (001) $ZnSiAs_2$ grown on (100) Ge using Auger spectroscopy for the purpose of looking for carbon and oxygen impurities. The analysis revealed the presence of a 50Å thick oxide layer on the $ZnSiAs_2$*. No oxygen was detected below 150Å. This provides the first direct evidence for and measure of the thickness of an oxide layer on $ZnSiAs_2$.

In summary, the buffered HF etch, which was intended to remove the oxide, did indeed improve the ohmicity of the contact, but in each case, it resulted in a substantial increase in the resistance near the origin (e.g. from ≃9KΩ to ≃260KΩ). At this time, the V-I characteristics of Figure 4 remain unexplained.

2.4 Carrier Concentration Measurements

Hall Effect measurements were made on $ZnSiAs_2$ layers grown under the same conditions that led initially to the identification of n-$ZnSiAs_2$ using Hall Effect and C-V measurements as described in the previous quarterly. This time, however, they were grown on α-Al_2O_3 and/or p-Si substrates in order to eliminate the substrate contribution to the Hall Effect measurements. The following table lists the results of Hall Measurements made on $ZnSiAs_2$ grown on these substrates.

---

*Measurements performed by courtesy of Dr. Charles K. Sinclair, Stanford Linear Accelerator Center, Stanford, Calif.

Table 1. Summary of Hall Measurements for $ZnSiAs_2$ Layers Grown on Substrates Indicated in Table.

Sample #	Substrate	(cm^3/Coul) Hall Coeff.	(cm^2/V-sec) Hall Mobility	(cm^{-3}) Carrier Conc.
OM91B	p-Si(15Ω-cm)	-949.3	25.4	6.58×10^{15}
OM92D	p-Si(15Ω-cm)	-257.4	22.6	2.43×10^{16}
OM90C	α-Al_2O_3	135.2	0.21	4.62×10^{16}
OM91C	α-Al_2O_3	-206.3	2.01	3.03×10^{16}
OM92E	α-Al_2O_3	32.2	0.727	1.94×10^{17}

The Hall data for samples OM91B, OM92D, and OM91C again indicate n-$ZnSiAs_2$ but with very low mobilities. This was especially true of the growth on the sapphire (α-Al_2O_3) substrate. Also of interest was that p-type material was obtained on samples OM90C and OM92E which exhibited extraordinarily low mobilities, almost indicative of a glassy deposit. The low mobilities in both cases are believed to be due in part to the poor morphology of the growth obtained on the Si and α-Al_2O_3 substrates and to the poly-crystalline nature of these deposits. Hall Effect data has not yet been taken on the recently obtained epitaxial deposits grown on Si and α-Al_2O_3 substrates. The epitaxial deposits are expected to show somewhat higher mobilities than the previously measured values from the poly-crystalline deposits.

The n-type deposits obtained on p-Si substrates as indicated by the Hall data seems to confirm the existence of n-$ZnSiAs_2$ and appears to eliminate the possibility of substrate interference in the Hall measurements. Good electrical isolation was seen between the epi-layer and the substrate (see Fig. 6). However, it is not clear yet whether this is due to a diffused layer in the Si as was the case for $ZnSiAs_2$ grown on GaAs. If a diffused layer exists, then it could render these conclusions invalid. This sample will be examined with EBIC in order to resolve this question.

The growth on α-Al_2O_3 substrates have provided the best evidence to date of the existence of low carrier concentration p- and n-$ZnSiAs_2$ (see data in Table 1). The low Hall mobilities for both conductivity types are very low and appear to be unique to the growth on α-Al_2O_3.

2.5 n-$ZnSiAs_2$/p-Si Structure

The Hall Effect sample, which was fabricated from OM91B using a Van der Pauw configuration, was also found to exhibit photovoltaic behavior (see Table 1 for results of Hall Effect measurements on this sample) although this sample was not intended for that purpose. The V-I curves shown in Figure 6 were originally intended to verify that isolation was achieved between the n-$ZnSiAs_2$ and the p-Si substrate. However, as can be seen, there is evidence of photovoltaic behavior when the sample is illuminated. There also appears to be some evidence for photoconduction as the illuminated forward curve has rotated inside the dark forward curve. It is unclear at this time if this is a true n-$ZnSiAs_2$/p-Si heterostructure or due to a diffused junction in the p-Si substrate. This sample will be examined using the EBIC technique before any further testing is performed.

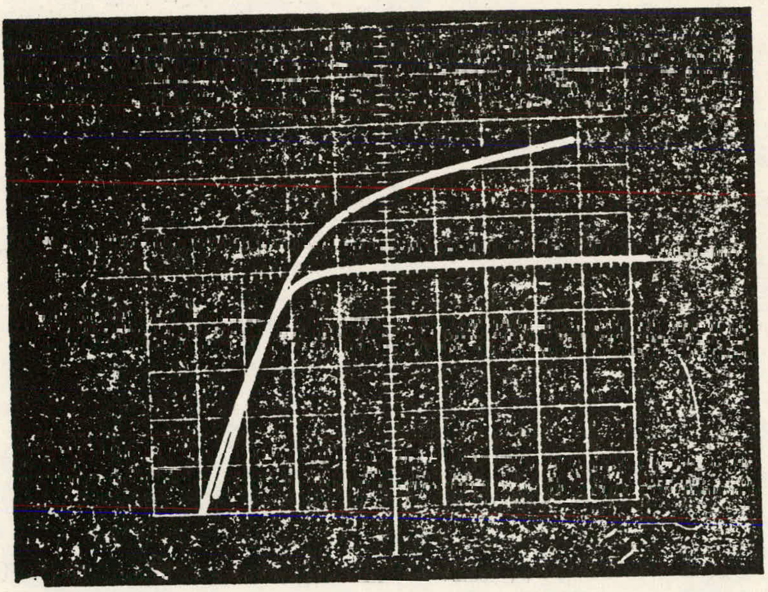

OM91B
n-$ZnSiAs_2$/p-Si

.1ma/div
.2v/div
Simulated AMO illum.
(High Press Xenon Lamp
with H_2O filter)

Figure 6. I-V curves for n-$ZnSiAs_2$/p-Si structure shown under AMO illumination (simulated with High Pressure Xenon Lamp with H_2O filter). Some evidence of photoconduction is evident from the reversal of the Forward Dark and AMO curves under high forward bias. Also evident is the effect of both high series and low shunt resistances.

2.6 $ZnSiAs_2$ p-n Junction Fabrication Effort

Several attempts have been made to fabricate $ZnSiAs_2$ p-n junctions on Si substrates using the stoichiometric deviation doping approach. Thus far, p-n junction behavior has not been seen and a secondary problem has arisen. To begin with, microscopic pin holes have been observed in some of these structures. Secondly, the process of etching mesa structures has revealed what appears to be cracks or grooves in the underlying substrate although unetched $ZnSiAs_2$ layer(s) have not shown any tendency toward cracking. Thus far, this seems to be characteristic only of layers grown abruptly on as-polished substrates. Further evaluations of these layers are planned in order to determine the origin of the cracks (or grooves) resulting in the substrate after mesa etching.

3.0 Planned Effort

Planned effort includes additional attempts to fabricate $ZnSiAs_2$ p-n junctions. The doping approach to be used will be S-doping using a H_2S dopant source.

Additional work is planned to determine the cause of the cracks (or grooves) in the Si substrate revealed by the mesa etching process.

☆U.S. GOVERNMENT PRINTING OFFICE: 1980-740-145/1135